On Interface Crack Growth and the Criterion to Determine the Direction of Ductile Crack Propagation

S. Hao, W. Brocks, M. Koçak, K.-H. Schwalbe

Institute of Materials Research, GKSS Research Center, D-21502 Geesthacht, Germany

ABSTRACT

Experimental research reveals that the dominant micromechanisms of ductile fracture are: 1) tearing due to highly localized shear strain 2) accumulation of damage in the form of void nucleation, growth and coalescence and 3) the combination of 1) and 2). An initial criterion for crack growth under mixmode loading has been suggested based on the GURSON-TVERGAARD-NEEDLEMAN (GTN) damage model that reflects the mutual effects of the Von Mises shear yield criterion and Rice-Tracy void growth law on the material yield surface.

The ductile crack growth behaviour (J-Δa or CTOD-Δa curves) at the interface between materials mismatched in yield strength has been investigated. The following conclusions have been drawn: Firstly, the slip-line field solution reveals that a higher stress triaxiality always takes place on the softer material side because of the discontinuity of transverse stresses over the interface. Secondly, both experimental results and numerical simulations using the GTN model indicate that a crack may grow along the interface or deviate into the softer material. Three factors, namely the global constraint, the hardening properties of the softer material and the distance between the crack tip and the interface strongly affect the direction of crack growth and the resistance against fracture.

INTRODUCTION

It has been observed experimentally that two kinds of failure micromechanisms may dominate the process of ductile fracture, i. e. shear tearing caused by highly localized strain and damage accumulation in the form of void nucleation, growth and coalescence. Thus, for a crack under mixmode loading, the classical criterion based on a non-damaged stress-strain field is no longer applicable because this kind of criterion cannot reflect the effect of damage on the ductile failure process.

Bimaterial systems with a mismatch of yield strength are frequently found in engineering practice. If a crack or a defect is located near or just at the interface between the two different materials the crack tip will be under local mixmode loading because of mismatch, and its resistance curve will obviously differ from the homogeneous case. It is of practical importance to determine the effect of mismatch on the resistance capacity of the interface crack.

Much effort has been concentrated on the interface crack problem in the last decade, both theoretically [1-10] and experimentally [11-17]. Figs. 1a, b show the process of microvoid coalescence during growth of an interface crack in an electron beam welded bend specimen made from austenitic 361L and P91 steels [17]. Continuing crack extension along the interface can be expected. Fig. 2 displays the crack growth profile in a M(T) specimen of StE 460 [17] in which the crack deviated from the interface and the crack growth path is dominated by a global shear band. It is therefore of vital importance to establish the criterion for mixmode crack growth and to specify the effect of mismatch on the fracture toughness of interface cracked bimaterial systems. The current investigation has been focused on this problem and the main results and some basic conclusions are presented in this paper.

THE CRITERION

For a homogeneous metal without damage the onset of plastic deformation is determined when the octahedral shear stress σ_e (i. e. the equivalent stress) reaches the value of the yield stress σ_Y (Von-Mises criterion):

$$\sigma_e / \sigma_Y = 1 \tag{1}$$

Rice and Tracy [18] have obtained the law of void growth from the solution of a single spherical void in an infinite perfectly-plastic body:

$$\frac{\dot{R}}{R} \propto \dot{E}^p \exp\left[\frac{3\sigma_m}{2\sigma_Y}\right] \tag{2}$$

where R, σ_m and E^p denote the radius of the void, the hydrostatic tensile stress and the plastic portion of macroscopic strain. Assuming that at the instance when the infinite body becomes plastically unstable the following relation exists:

$$\frac{\dot{R}}{R\dot{E}^p} \propto f$$

where f is the volume fraction of the void; then combining (1) and (2) gives

$$\left(\frac{\sigma_e}{\sigma_Y}\right)^m + f \cdot \exp\left(\frac{3\sigma_m}{2\sigma_Y}\right) - \left(1 + qf^2\right) = 0 \tag{3}$$

where m and q are constants.

Based on the solution of cell models, Gurson has obtained a general yield criterion [19] which has been further developed by Tvargaard and Needleman [20-22]. This criterion, hereafter refered to as the GTN model, is expressed as:

$$\Phi(\sigma_e, \sigma_m, \sigma_Y, f^*) = \frac{\sigma_e^2}{\sigma_Y^2} + 2q_1 f^* \cosh\left(q_2 \frac{3\sigma_m}{2\sigma_Y}\right) - \left(1 + q_3 f^{*2}\right) = 0 \tag{4}$$

where q_1, q_2, q_3 are constant; f^* is a function of f which reflects the acceleration of void growth after coalescence and σ_Y is the actual flow stress of the matrix material. The expressions for $f(f^*)$ and the damage evolution equations are listed in the Appendix. Comparing (3) with (4) one may conclude that the GTN yield criterion determines the onset of unstable plastic deformation caused by either shear yielding or void nucleation, growth and coalescence or a combination of the two mechanisms.

According to (4) macroscopic crack growth occurs when a certain value of f is exceeded in a material element, so that the GTN yield surface in this element degenerates to a point (see Fig. 3) and the element loses its stress carrying capability. Using the subscript "$f=0$" to denote the value of the quantities which exist in the undamaged state (f=0), the reduction of the yield surface can be specified by the parameter S_Y, as illustrated in Fig. 3. Obviously, S_Y is a function of f and its value can be determined by solving the equation below:

$$\left(\frac{\sigma_{e,f=0}}{\sigma_Y} S_Y\right)^2 + 2q_1 f^* \cosh\left(q_2 \frac{3S_Y \sigma_{m,f=0}}{2\sigma_Y}\right) - \left(1 + q_3 f^{*2}\right) = 0 \tag{5}$$

Thus a crack will grow along the direction on which the material element has the smallest yield surface, in other words, that which has the lowest value of S_Y. In a polar co-ordinate system $\{r,\theta\}$ which originates at the crack tip, the criterion to determine the angle of the crack growth direction θ_{growth} can be expressed by:

$$\theta_{growth} = \theta\left\{S_Y|_{r=l_0} = min\left[S_Y|_{\theta,r=l_0}\right]\right\} \tag{6}$$

where l_0 is a material constant, and the initial crack growth criterion is

$$S_Y|_{\theta=\theta_{growth},r=l_0} = 0 \tag{7}$$

THE SIMULATION OF INTERFACIAL CRACK GROWTH

Crack Tip Stress-Strain Field

If the stress-strain and damage fields surrounding a crack tip are well known, then using (6) and (7) one may determine the crack growth direction. In the present work the analytical solutions for a crack at the interface between dissimilar perfectly-plastic materials with a mismatch in yield strengths, M

$$M = \frac{\sigma_Y^I}{\sigma_Y^{II}} \tag{8}$$

are established. The superscripts „I" and „II" denote the respective quantities in either material. Assuming elastic perfectly-plastic material behaviour, the general boundary conditions and the resulting equations for the stress components over an interface between perfectly-plastic materials have been established in [8]. It was concluded that a discontinuity of transverse stress existed over the interface. In the weaker material side (denoted as material "I") the transverse stress and thus the mean stress σ_m,(hydrostatic stress) were higher than in material "II". In the case of the load being normal to the interface this difference is given by the following relation:

$$\sigma_m^I - \sigma_m^{II} = \frac{\sigma_Y^{II} - \sigma_Y^I}{\sqrt{3}} \tag{9}$$

The slip-line field for an interface crack tip under small scale plane strain yielding conditions has been constructed (as shown in Fig. 4a), assuming that no friction exists on the crack traction-free surface. In the softer material side, the slip-line field consists of two uniform fields A and C of constant stress and a central fan B in which the stresses vary proportionally to the angle θ. In the harder material side an additional elastic wedge G may emerge (Fig. 4a). The slip line fields are determined by the five variables: θ_1, θ_2, θ_3, θ_4, θ_5 which are functions of the degree of mismatch (M), the boundary conditions of the crack wedge and the value of transverse stress. A group of solutions are given in Fig. 4b. From this diagram one sees that the size of fan B (the angle θ_1) increases as the value of M decrease. In the case of M=0.707 the constant stress zone C disappears with $\theta_1 = 3\pi/4$. The elastic wedge G is present only when M≤0.707 or when the transverse stress is very low. It can be concluded that when M≤0.707 the stress distribution in the softer material is constant and independent of the degree of mismatch.

From the slip-line field in Fig. 4a one cannot evaluate S_Y using equations (5-7) because these solutions provide only the stress distribution, but the evolution of damage depends on the distribution of strain increments. The kinematic velocity fields for two geometries (single and double edge tensile panels with a middle interface) have been obtained and are shown in Fig.

5. Neglecting the effect of coupling between damage and the slip-line field, the values of S_Y have been calculated under initial loading conditions and are shown in Fig. 6. From this diagram one may anticipate that in the single edge panel the crack will grow along the direction of the shear strain localization band while in the double edge panel the crack will grow along the interface because of high constraint.

The slip-line field in Fig. 4a also predicts no local crack blunting directly ahead of the tip. Assuming that the profile of a blunted crack tip is constant during deformation, the resulting change of the slip line field in Fig. 4a is shown in Fig. 7. It can be seen that the constant stress regions A and C in the softer material remain, and the fan region B focuses intense strains into the region "**abc**" directly ahead of the blunted tip. On the other hand plastic deformation is hindered in the region "**acd**" by the harder material below the interface, which induces a high stress triaxiality. The maximum stresses appear at the point "**d**". If M is less than 0.707 we can obtain the stress at this point:

$$\sigma_{11} = \sigma_{22} = \sigma_m^I = \frac{\sigma_Y^I}{\sqrt{3}}\left(1 + \frac{3\pi}{2}\right) \tag{8}$$

For the blunted crack tip in Fig. 7 full scale yielding is achieved when an intensely localized strain develops along the slip-line "**ac**" and connects to a global shear band, similarly to the case in Fig. 5a. Thus an interface crack may grow in two ways: straight along the interface due to the high stress triaxiality described by (8) or deviated into the softer material along the line "**ac**".

Numerical Simulation

The GTN model described has been implemented as a user supplied routine [23] in the FE program ABAQUS. Crack growth behaviour for different 2D and 3D geometries and degrees of mismatch have been simulated and details of the results are given in [24]. Displayed in Fig. 8 are group of J-Δa curves, the corresponding crack growth profiles and the contours of stress are shown in Fig. 9. Fig. 10 shows the simulation of interfacial crack growth in a 3D thin M(T) specimen, in which the crack grows deviated from the interface. It has been concluded that an interface crack always grows in the softer phase if no debonding takes place. The crack may grow straight along the interface, but under certain conditions it may deviate from the interface into the softer material. High global in-plane or out-of-plane constraint and strong strain hardening keep the crack growing straight along the interface. According to the slip-line solution the distance between the crack tip and the interface determines the level of stress triaxiality and thus strongly influences the resistance to fracture. If the crack path is crooked, it is a fundamental question for practical applications to correctly define Δa and the fracture resistance.

CONCLUDING REMARKS

Taking into account the two micromechanisms of ductile fracture, criteria for determining initial crack growth and direction under mixmode loading have been suggested based on the GTN model. The analyses have demonstrated that the GTN model is a very powerful method for the simulation of ductile crack growth at the interface of mismatched materials. Combining experimental investigations with computational methods will prove to be effective in future engineering design and integrity assessment.

APPENDIX [20-22]

In (9) the modified damage parameter f^*

$$f^* = \begin{cases} f & \text{for } f \le f_c \\ f_c + K(f - f_c) & \text{for } f > f_c \end{cases} \qquad \text{with } K = \frac{f_u^* - f_c}{f_f - f_c} \tag{A1}$$

accounts for the accelerated process of coalescence after reaching a critical void volume fraction f_c [19]. The equation for the evolution of f generally consists of two terms describing the nucleation and growth

$$\dot{f} = \dot{f}_{growth} + \dot{f}_{nucl} \quad ; \qquad f|_{t=0} = f_0 \tag{A2}$$

with

$$\dot{f}_{growth} = (1 - f)\dot{\boldsymbol{\varepsilon}}^p : \boldsymbol{I} \tag{A3}$$

and

$$\dot{f}_{nucleation} = \dot{\varepsilon}^p A_1 + (\dot{\sigma}_m + \dot{\sigma}_e) A_2 \tag{A4}$$

where ε^p is the equivalent mesoscopic plastic strain.

REFERENCES

[1] WILLIAMS, M. L., „The stresses around a fault or crack in dissimilar media", Bulletin of the Seismological Society of America 49 (1959), pp. 199-204.

[2] COMNINOU, M. and SCHMUESER, D.: „The interface crack in a combined tension-compression and shear field", ASME, J. of Appl. Mech. 46 (1979), pp. 345-348.

[3] HUTCHINSON, J. W., MEAR, M., and RICE, J. R.: „Crack paralleling an interface between dissimilar media", ASME, J. of Appl. Mech. 54 (1987), pp. 828-832.

[4] RICE, J. R., „Elastic fracture mechanics concepts for interfacial cracks", ASME, , J. of Appl. Mech. 55 (1988) pp. 418-423.

[5] SHIH, C. F. and ASARO, R .J.: „Elastic-plastic analysis of cracks on bi-material interfaces,; Part I: small scale yielding", ASME, J. of Appl. Mech. 55 (1988), pp. 299-316.

[6] SHIH, C. F. and ASARO, R. J.: „Elastic-plastic analysis of cracks on bi-material interfaces,; Part II: structures of small scale yielding field ", ASME, J. of Appl. Mech. 56 (1989), pp. 763-779.

[7] SHIH, C. F. and ASARO, R. J., „Elastic-plastic analysis of cracks on bi-material interfaces,; Part III: large scale yielding", ASME, J. of Appl. Mech. 58 (1991), pp.450-463.

[8] HAO, S., CORNEC, A. and SCHWALBE, K.-H.: „Plastic stress-strain fields and limit loads of a plane strain cracked tensile panel with a mismatched welded joint", to be published in Int. J. of Solids & Structures.

[9] HAO, S., CORNEC, A. and SCHWALBE, K.-H.: „A Compilation of Solutions for Limit Load and constraint for 2D specimens", 2nd Int. Symp. on Mis-Matching of Welds, Reinstof, Germany, April 1996

[10] ZYWICZ, E. and PARKS, D. M., „Small-scale yielding interfacial crack tip fields", J. Mech. Phys. Solids, 40 (1992), pp. 511-536.

[11] TSCHEGG, E. K. KIRCHNER, H. O. K., and SCHWALBE, K. -H., „Cracks at interface of different cohesion", Acta Met. Mater.

[12] EPSTEIN, J. S. et. al., „Elastic-plastic crack tip fields for bimaterial interface and interleaf geometries", Mis-Matching of Weld, ESIS Pub.17, 1993, pp. 265-280.

[13] HERRMANN, K. P. and GREBNER, H., „Curved thermal crack growth in nonhomogeneous materials with different shaped external boundary", I. Theoretical

results, II. Experimental results", Theoret. Appl. Fracture Mech., V.2, 1984, pp. 133-155.

[14] MEYER, M. and SCHMAUDER, S., „Thermal stress intensity factors of interface cracks in bimaterials", Int. J. of Fracture, V.57, 1992, pp. 381-388.

[15] REIMANIS, I. E., et. al. „Effects of plasticity on the crack propergation resistance of a metal/ceramic interface", V.38, 1990, pp. 2645-2652.

[16] EVANS, A. G. and DALGLEISH, B. J., „The fracture resistance of metal-ceramic interfaces", Acta Met. Mater., V.40, 1992, pp. S295-S306.

[17] Koçak, M., Es-Souni, M., Chen, L. and K.-H. Schwalbe, „Microstructure and weld metal matching effects on HAZ toughness", Proceeding of the 8th Int. Conf., OMAE-89, Vol.III, 1989.

[18] RICE, J. R. and TRACEY,:D.M. „On the ductile enlargement of voids in triaxial stress fields", J. Mech. Phys. Solids 17 (1969), 201-217.

[19] GURSON, A.L., J. Engng. Mat. Techn. V. 99, 1977, pp. 2- 15.

[20] TVERGAARD, V,: "Influence of Voids on Shear Band Instabilities under Plane Strain Conditions", Int. J. of Fract.. 17 (1981), pp. 389-407.

[21] NEEDLEMAN, A., and TVERGAARD., J. Mech. Phys. Solids. V. 35, 1987, pp. 151-.183.

[22] NEEDLEMAN, A., and RICE, J. R., „Limits to ductility set by plastic flow localization", Mechanics of sheet metal forming, D. P. Koistinen et al. eds., 1978, pp. 237-267.

[23] HAO, S. and BROCKS, W.: „The GURSON TVERGAARD NEEDLEMAN model for temperature and rate dependent material with isotropic und kinematic hardening", Technical Note GKSS/WMG/95/1, GKSS Research Centre (1995).

[24] HAO, S., BROCKS, W., Koçak, M. and SCHWALBE, K.-H.: „On the Stress-Strain field and damage evolution at a fusion line (interface) crack tip", GKSS Tech. Note and presented in the 2nd Int. Symp. on Mis-Matching of Welds, Reinstof, Germany, April 1996.

a) Overview

b) Crack tip local

Fig. 1 Crack growth by void coalescence at an interface in a SE(B) specimen

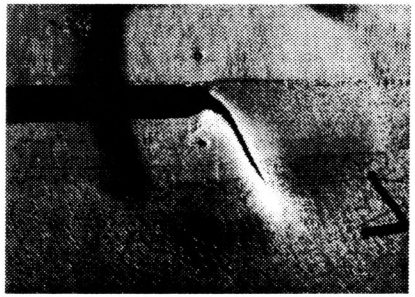

Fig. 2 The crooked path of crack growth at the interface in a M(T) specimen

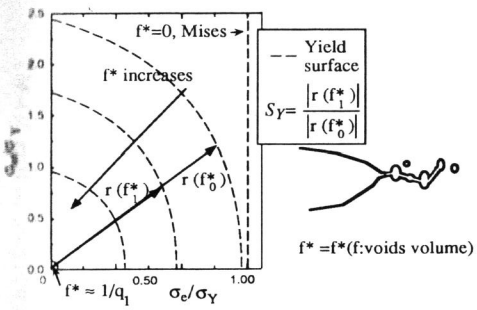

Fig. 3. Schematic of the yield surface introduced by GTN model

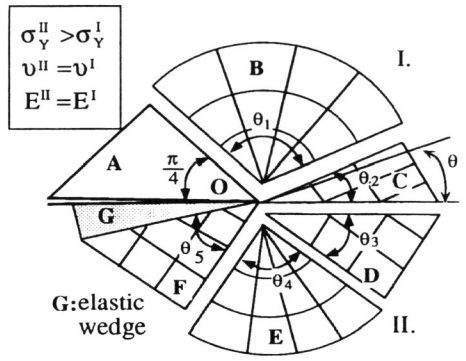

Fig. 4a The structure of the crack tip field

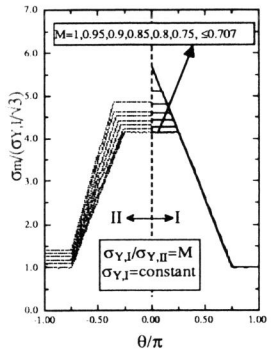

Fig. 4b Jumping of triaxiality over interface

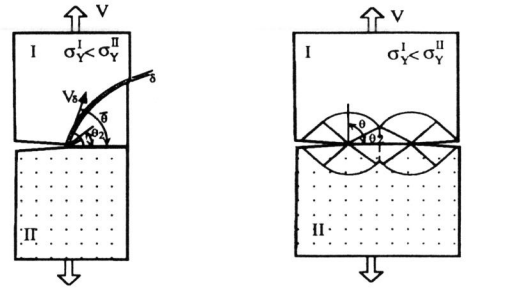

a) Double Edges Tensile Panel {DT(E) }

b) Single Edge Tensile Panel {S(E)}

Fig. 5 The kenimatical velocity fields for two geometries

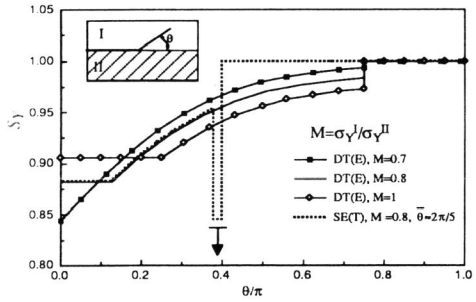

Fig. 6 Prediction of the Sy surround the crack tips

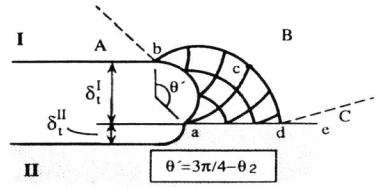

Fig. 8 Slip-line field in the blunted crack tip region in the side of softer material

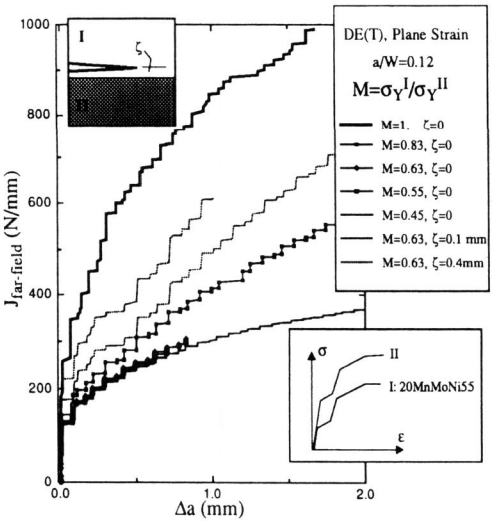

Fig. 8 A Group of resistance curves of interlayer crack

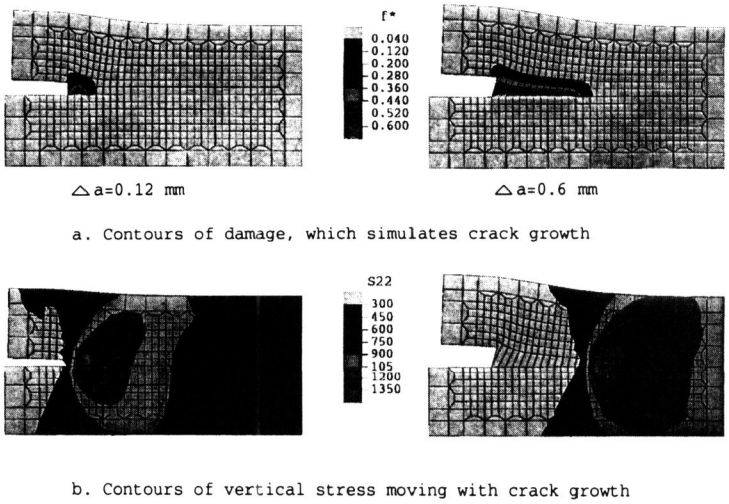

Fig.9 An on interface growing crack tip simulated by GTN model

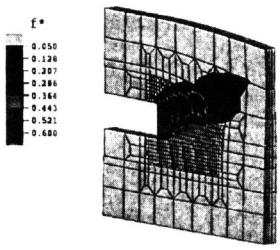

Fig.10. The interface crack growth path of thin 3D-MT